IN-VENTO 2026
International Conference of the Italian Association for Wind Engineering
Bari, September 13th – 16th, 2026

Multi-level high-resolution wind-seismic hazard maps

Lorenzo Raffaele[a] and Luca Bruno[a]

[a]*GeoWindy R&D Group, Department of Architecture and Design, Politecnico di Torino, Torino, Italy, lorenzo.raffaele@polito.it, luca.bruno@polito.it*

SUMMARY:
This study proposes a novel multi-level framework for high-resolution comparative mapping of wind and seismic hazards. The modelling framework integrates different hazard intensity measures into a multi-dimensional intensity index to quantify both the combined magnitude and prevalence of hazards across wide geographic regions. The framework is structured into three levels of increasing specificity: (i) mapping solely based on the hazard, (ii) aggregated fragility-aware mapping for classes of structures, and (iii) fragility-aware mapping for specific structures. Lattice towers for power transmission lines are adopted as a benchmark application. The resulting maps over the Calabria region are critically assessed and compared with multi-risk mapping to highlight approximations introduced by each level of increasing specificity.

Keywords: wind, earthquake, hazard, vulnerability, mapping, lattice towers

1. INTRODUCTION

Wind and seism are among the most relevant environmental actions governing the design of structures subjected to loads with prevailing horizontal force components. Traditionally, structural safety has been addressed within the Load-and-Resistance-Factor Design (LRFD) framework. Since the 1990s, Performance-Based Earthquake Engineering (PBEE) has been developed as an alternative paradigm, providing a comprehensive probabilistic framework that explicitly links seismic hazard, asset's exposure and structural vulnerability (Porter, 2003).
Within PBEE, hazard analysis represents the first and crucial ring of the methodological chain. Over the past decades, extensive efforts have produced seismic hazard maps based on the Probabilistic Seismic Hazard Analysis (PSHA) approach introduced by Cornell, 1968. These maps have been developed at national (e.g. in Italy, Meletti et al., 2006), regional (e.g. Europe, Danciu, Giardini, et al., 2024), and global (e.g. Johnson, Villani, et al., 2023) scales with progressively increasing spatial resolution (e.g. $\Delta\varphi = \Delta\lambda = 0.02°$ in Italy).
Inspired by PBEE, Performance-Based Wind Engineering (PBWE) was introduced in the early 2000s (Ciampoli et al., 2011). However, the development of PBWE has long been limited by the lack of high-resolution wind hazard maps. In conventional wind design, wind loads are commonly characterized through the estimation of the design wind speed, a key element of the so-called Alan G. Davenport Wind Loading Chain (Picozzi et al., 2024). National climatic maps have therefore been developed in several countries. In Italy, for example, wind maps have been available since Ballio et al., 1999 and have recently been updated by Ricciardelli et al., 2025. Recently, Raffaele et al., 2024 introduced a high-resolution ($\Delta\varphi = \Delta\lambda = 0.02°$) omnidirectional wind-speed mapping approach based on the Very High Resolution dataset developed by CMCC (Raffa, Reder, et al., 2021), obtained through the dynamical downscaling of ERA5 reanalysis data, enabling consistent comparisons between wind and seismic hazards.
The present study proposes a compact mapping approach to compare wind and seismic hazards, with the perspective of extending the framework to additional natural hazards. Lattice towers supporting overhead power transmission lines are adopted as a benchmarking structural typology due to their extensive territorial coverage, critical role within power infrastructures, documented vulnerability to wind and seismic hazards, and high degree of standardization.

2. MODELLING APPROACH

Even if the present study focuses on wind and seismic hazards, in the following we propose a general framework for the comparative mapping of n generic hazards. Analogously, even if this study refers to the fragility of power line lattice towers, the general framework is applicable to a wide range of exposed structures and infrastructure systems.

Let us assume that each i-th hazard is quantified by its Intensity Measures IM_i. For instance, for n=2, $IM_1 = U$ $[m/s]$ being U the mean wind speed, and $IM_2 = PGA$ $[m/s^2]$ being PGA the Peak Ground Acceleration. Each $IM_i(\varphi, \lambda)$ is mapped over a given geographical domain Ω, where φ and λ are the latitude and longitude, respectively. The maps should have the same spatial resolution $(\Delta\varphi, \Delta\lambda)$ if interpolation is to be avoided, but not necessarily refer to the same return period T_{Ri} associated to the i-th IM. In the above 2D case ($IM_1 = U$, $IM_2 = PGA$, $T_{R1} = 50$ years, $T_{R2} = 475$ years), we can define the $U_{50} - PGA_{475}$ plane.

Let us set a reference value IM_{Ri} for each IM_i over Ω. The normalized dimensionless measure IM_i^* of each IM_i with respect to its reference value IM_{Ri} reads as

$$IM_i^*(\varphi, \lambda) = \frac{IM_i(\varphi, \lambda)}{IM_{Ri}}, \quad IM_i^* \in [0, +\infty[\tag{1}$$

i.e. it defines its Cartesian coordinate in the n-dimensional hazard Euclidean hyperspace. In the above 2D case ($IM_1 = U$, $IM_2 = PGA$) it reduces to the $U_{50}^* - PGA_{475}^*$ plane. The module of the distance R from the origin $0(0,...,0)$ generally reads

$$R(\varphi, \lambda) = \left| \sqrt{IM_n^{*2} + IM_{n-1}^{*}{}^{2} + ... + IM_2^{*2} + IM_1^{*2}} \right|, \quad R \in [0, +\infty[\tag{2}$$

The proposed Multi-Dimensional Intensity Index (MDII) is generally defined in the same hazard hyperspace by referring to the generalized spherical coordinates defined by classical transformation from the Cartesian ones together with the translation of the origin in the point $O(1,...,1)$, i.e. one radial coordinate r

$$r(\varphi, \lambda) = \left| \sqrt{(IM_n^* - 1)^2 + (IM_{n-1}^* - 1)^2 + ... + (IM_1^* - 1)^2} \right|, \quad r \in [0, +\infty[\tag{3}$$

and n-1 angular coordinates θ_i

$$\theta_i(\varphi, \lambda) = \text{atan2}\left[\sqrt{(IM_n^* - 1)^2 + (IM_{n-1}^* - 1)^2 + ... + (IM_{i+1}^* - 1)^2}, (IM_i^* - 1) \right], \tag{4}$$

where atan2 is the two-argument arctangent function, $\theta_i \in [0, \pi]$ $\forall i = 1...n-2$ and $\theta_{n-1} \in [-\pi, \pi]$. In the above 2D case, the polar coordinates in the hazard plane merely reduce to $r(\varphi, \lambda) = \left| \sqrt{(PGA_{475}^* - 1)^2 + (U_{50}^* - 1)^2} \right|$, and $\theta(\varphi, \lambda) = \text{atan2}\left(PGA_{475}^* - 1, U_{50}^* - 1\right)$. The angular coordinate θ allows to map the hazard hyperspace by identifying the prevailing hazard and if they are above or below reference. In the above 2D case, we can distinguish among: $0 < \theta < \pi/4$, both hazards are above reference, the wind one prevails ($U^* > PGA^* > 1$); $\pi/4 < \theta < \pi/2$, both hazards are above reference, the seismic one prevails ($PGA^* > U^* > 1$); $\pi/2 < \theta < \pi$, the seismic hazard is above reference, the wind one below ($PGA^* > 1, U^* < 1$); $-\pi < \theta < -3/4\pi$, both hazards are below the reference value, but the seismic one prevails ($U^* < PGA^* < 1$); $-3/4\pi < \theta < -\pi/2$, both hazards are below reference, but the wind one prevails ($PGA^* < U^* < 1$); $-\pi/2 < \theta < 1$, the wind hazard is above reference, the seismic one below ($U^* > 1, PGA^* < 1$).

The proper choice of the reference values IM_{Ri} clearly plays a crucial role in such a framework. Such a choice is not unique, and can secure the desired flexibility to the general framework, by selecting reference values relevant to different engineering goals. In the following, three levels are detailed in ascending order of specificity but, also in decreasing order of generality.

2.1. Level 1 - Multi Hazard Comparative Mapping

Level 1 is intended to compare two or more hazards without any reference to structural vulnerability. The reference value IM_{Ri} over the considered domain Ω can be set equal to a suitable p-th percentile of IM_i , e.g. the median value $IM_{50,i}$, or a reference value for specific return periods in standards, e.g. the reference PGA on rock a_{gR} defined in EN-1998-1:2004, 2004, and the reference base wind velocity at sea level $U_{b,0}$ defined in EN-1991-1-4:2005, 2010. Hence, in Level 1 the above generic wording 'reference' can be replaced by 'percentile', or alternatively by 'codified value'. The resulting mapping is potentially of interest for National public authorities, e.g. the Italian Civil Protection, in order to characterize wide areas of land irrespectively of the exposed asset.

2.2. Level 2 - Aggregated Fragility-Aware Multi Hazard Comparative Mapping

In Level 2 the IM_{Ri} is the hazard conventional damaging threshold value corresponding to a suitable probability of failure. It can be obtained as the IM value corresponding to a given probability of exceeding a specific damage state according to an aggregated fragility curve, e.g. an ensemble-average $\overline{P}_{Fi}$, i.e. $IM_{Ri} \mid \overline{P}_{Fi} = P_{Fi,th}$. $\overline{P}_{F,i}$ refers to a given structural type, e.g. bridges along highways or railways (Crespi et al., 2025). Hence, in Level 2 the above wording 'reference' can be replaced by 'aggregated damaging value'. The resulting mapping is of potential interest for owners or operators of large networks stretched on vast territories, e.g. national or transnational railway/highway agencies, power transmission companies, in order to plan and prioritize maintenance or retrofitting, construction or relocation of the assets.

2.3. Level 3 - Fragility-Aware Multi Hazard Comparative Mapping

Analogously to Level 2, IM_{Ri} is defined as $IM_{Ri} \mid P_{Fi} = P_{Fi,th}$, but obtained with reference to the single fragility curve of a specific structure. Hence, in Level 3 the generic wording 'reference' can be replaced by 'specific damaging value'. The resulting mapping is potentially of interest for the design of structures that cannot be ascribed to a recurrent structural type, or more generally to focus on a specific structure.

3. PRELIMINARY RESULTS

In Figure 1, some preliminary results are included to show a glimpse of the potentialities derived from the adoption of the proposed multi-level multi-hazard comparative mapping. In particular, Figure 1(a,b) shows the wind and seismic hazard maps, while Figure 1(c) shows the Level 1 wind-seismic hazard map over Calabria assigning codified values as reference ones. Level 1 mapping clearly defines in synthetic terms most hazardous regions by providing the degree prevalence of each hazard θ (filled contour) and their combined normalized intensity R (isocontour lines). The resulting comparative hazard maps over the region will be critically assessed for each level and compared with multi-risk maps to highlight the approximations introduced by each level of increasing specificity.

ACKNOWLEDGEMENTS

This study was jointly carried out within the RETURN Extended Partnership and received funding from the European Union Next-GenerationEU (National Recovery and Resilience Plan – NRRP, Mission 4, Component 2, Investment 1.3 – D.D. 1243 2/8/2022, PE0000005) – SPOKE TS 2; and the research project PROtection Technologies from Eolian Events for Coastal Territories (PROTEECT, http://www.proteect.polito.it/) within the Ministerial Decree no. 1062/2021 and received funding from the FSE REACT-EU - PON Ricerca e Innovazione 2014-2020. This manuscript reflects only the Author's views and opinions, neither the European Union

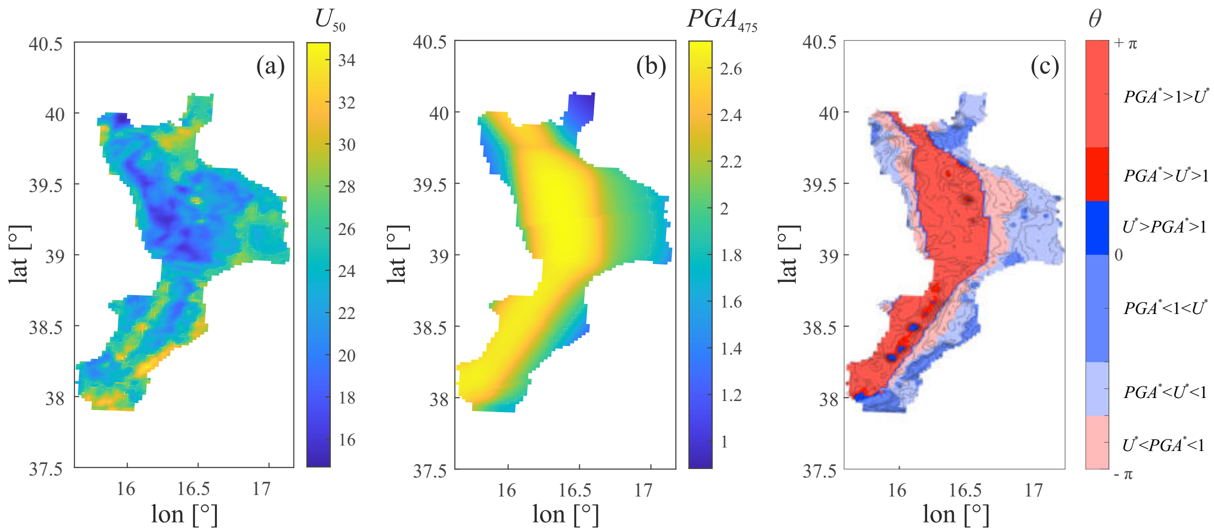

Figure 1. Wind hazard map (a) according to Raffaele et al., 2024, seismic hazard map (b) according to Meletti et al., 2006, resulting Level 1 - Multi hazard comparative mapping (c) over Calabria region.

nor the European Commission can be considered responsible for them.

REFERENCES

Ballio, G., S. Lagomarsino, G. Piccardo, and G. Solari (1999). Probabilistic analysis of Italian extreme winds: Reference velocity and return criterion. Wind and Structures 2, 51–68.

Ciampoli, M., F. Petrini, and G. Augusti (2011). Performance-Based Wind Engineering: Towards a general procedure. Structural safety 33, 367–378.

Cornell, C. A. (1968). Engineering seismic risk analysis. Bulletin of the Seismological Society of America 58, 1583–1606.

Crespi, P., M. Scamardo, and R. Buoninconti (2025). Fragility curves for the seismic vulnerability of a stock of Italian highway bridges. Structures 78, 109374.

Danciu, L., D. Giardini, et al. (2024). The 2020 European Seismic Hazard Model: overview and results. Natural Hazards and Earth System Sciences 24, 3049–3073.

EN-1991-1-4:2005 (2010). *Eurocode 1: Actions on structures - Part 1-4: General actions - Wind actions*. Standard. European Committee for Standardization, Brussels, Belgium.

EN-1998-1:2004 (2004). *Eurocode 8: Design of structures for earthquake resistance - Part 1: General rules, seismic actions and rules for buildings*. Tech. rep. European Committee for Standardization, Brussels, Belgium.

Johnson, K., M. Villani, et al. (2023). *Global Earthquake Model (GEM) Seismic Hazard Map (version 2023.1 - June 2023)*.

Meletti, C., V. Montaldo, M. Stucchi, and F. Martinelli (2006). *Database della pericolosità sismica MPS04*.

Picozzi, V., F. Landi, A. Avossa, P. Croce, P. Formichi, and F. Ricciardelli (2024). The Climatic Action Uncertainty Chain. Engineering Structures 301, 117357.

Porter, K. A. (2003). An overview of PEER's performance-based earthquake engineering methodology. Proceedings of ninth international conference on applications of statistics and probability in civil engineering. Vol. 52, 3729–3735.

Raffa, M., A. Reder, et al. (2021). VHR-REA_IT Dataset: Very High Resolution Dynamical Downscaling of ERA5 Reanalysis over Italy by COSMO-CLM. Data 6.

Raffaele, L., L. Bruno, and E. Colucci (2024). Reanalysis-based mesoscale wind maps for the design of structures and infrastructures with an application to Italy. Journal of Wind Engineering and Industrial Aerodynamics 253, 105844.

Ricciardelli, F., A. Akbaba, V. Picozzi, and A. Avossa (2025). An updated wind hazard map of Italy. Journal of Building Engineering 115, 114457.